# Salt-templated strategy for well dispersed multi-component composites with morphologies ranging from millimeter to nanoscale<sup>1</sup>

### Abstract

Typically agglomeration of multi-component composites is avoided by a combination of dispersion agents, and complex chemical strategies. This, however, is associated with complex procedures and high production costs. For the first time, an advanced procedure is presented for the homogeneous dispersion of multi-component titanium composites with morphologies ranging from millimeter to nano- scale (Al<sub>2</sub>O<sub>3</sub> fiber, SiC whisker, graphene and MXene), are achieved by this salt-templated strategy (STS) based on naturally abundant, water-soluble and recyclable NaCl crystals as templates. Salt templates aid retaining of the space/distance between different components and the 'ball milling agents'. The high homogeneity of the obtained composites before and after sintering is characterized and confirmed. Additionally, the salt templates are removed and recycled, no influence of the salt is expected for further applications. Hence, this work potentially paves ways for the mass production and application of multi-component composites with various morphologies for various applications.

Keywords: Salt; Template; Homogeneity; Composite

### 1. Introduction

Composites, which are composed of two or more distinct materials, have been developed to obtain different combined properties that are not found in the individual components [1]. Regarding reinforced composites, to date, various kinds of whiskers and fibers are commonly used to achieve such outstanding properties, such as SiC whiskers [2], Al<sub>2</sub>O<sub>3</sub> fibers [3] and others. However, one of the main challenges is still the dispersion of the fibers/whiskers, mainly due to their different morphologies. This is particularly challenging for nano-materials such as graphene or micro-materials owing to their tendency to agglomerate due to Van der Waals forces [4, 5], thereby resulting only in moderate enhancement in the mechanical, electrical, and/or thermal and other properties of the targeted composites [6].

To obtain a multi-component powder mixture with high homogeneity, several mechanical and chemical strategies were developed. For example, short fiber or whisker or carbon nanotube reinforced composites were obtained by high energy ball milling (HEBM) and ultra-sonication methods [7-9]. However, due to the formation of open edges, vacancies and defects in the short fibers, carbon nanotubes and graphene, constituting the non-sp<sup>2</sup> structural disorders during ball milling, unique properties were not achieved [10]. Moreover, some chemical strategies were efficacious to obtain high homogeneity but specific and complex [11-13]. Obviously, most of these methods summarized above require a long process cycle, hence, are laborious, and/or energy-intensive. The resulting high process costs have thus significantly constrained the scope of the application of composites. Therefore, novel, facile, possible environmentally friendly mixing technologies are highly desirable and have become an urgent, to be solved problem.

A templating method is commonly used to obtain porous structures with large specific surface areas, especially for the salt leaching [10, 14]. Predominantly, sodium chloride (NaCl) has been used as salt

<sup>&</sup>lt;sup>1</sup> Xiaoqiang Li <sup>a,1,\*</sup>, Xin Zhao <sup>a,1</sup>, Jesus Gonzalez-Julian<sup>b,c</sup>, Jürgen Malzbender<sup>a</sup>

<sup>&</sup>lt;sup>a</sup> Institute of Energy and Climate Research: Microstructure and Properties of Materials (IEK-2), Forschungszentrum Jülich GmbH, 52425 Jülich, Germany.

<sup>&</sup>lt;sup>b</sup> Institute of Energy and Climate Research: Materials Synthesis and Processing (IEK-1), Forschungszentrum Jülich GmbH, 52425 Jülich, Germany

<sup>&</sup>lt;sup>c</sup> Institute of Mineral Engineering, Department of Ceramics and Refractory Materials, RWTH Aachen University, 52062 Aachen, Germany

<sup>&</sup>lt;sup>1</sup> X. Li and X. Zhao contributed equally.

<sup>\*</sup> Corresponding author, e-mail: Xiaoqiang Li, xi.li@fz-juelich.de

template, because it is an abundant, cheap, and non-toxic template material that readily dissolves in water without the need of additional organic solvents.

Hence, in the current work, as an example, the homogeneously distributed multi-component titanium composites with morphologies ranging from millimeter to nano- scale (Al<sub>2</sub>O<sub>3</sub> fiber, SiC whisker, graphene and MXene), were prepared for the first time by this simple and environmentally friendly salt-templated strategy (STS). Those components are the representatives of the most investigated components with morphologies ranging from millimeter to nanometer scale. As a result, it offers a possibility to have a comparison with previous work and further improve them. Second, the graphene and MXene were selected due to various functional groups on the surfaces, thus it can also check the feasibility of this strategy without the further consideration of the functional groups. Therefore, Al<sub>2</sub>O<sub>3</sub> fiber, SiC whisker, graphene and MXene were selected as the main research objects in the current work. The salt-templated strategy is based on the retained distance/space and micromechanics by intercalation of removable salt particles during the stirring process. In addition, during this process, NaCl particles are used as the salt templates, and this salt is abundant in nature and cheap, and not harmful to the environment. And this salts can be recycled for sustainable procedure. Therefore, this strategy has the potential for the application if increasing the batch size or making the process continuous. Therefore, the process is environmentally friendly, sustainable and cost-saving, hence, with application relevant.

### 2. Material and methods

## 2.1. Preparation of the raw materials

The preparation of raw materials is described in supplementary material.

# 2.2. Mixing via salt-templated strategy (STS)

To illustrate the effectiveness and versatility of the NaCl STS, several experiments were designed and summarized in Table 1. For comparison, 10 vol. % Al<sub>2</sub>O<sub>3</sub> fibers were dispersed directly within titanium composites using ultrasound. Furthermore, NH<sub>4</sub>HCO<sub>3</sub> STS was applied to illustrate the potential further implementation to various approaches using different salts. The details of the experimental procedure is described as follows.

### 2.2.1. Millimeter material

First, Al<sub>2</sub>O<sub>3</sub> fibers were dispersed in ethanol in a beaker via ultrasound (VWR TM) to obtain a homogeneous dispersion. Then NaCl powders were poured into the beaker, with a ratio in volume NaCl powder to fibers of 50:1, followed by addition of Ti powders into the mixture of NaCl and Al<sub>2</sub>O<sub>3</sub> fibers. Afterwards, the mixture was magnetic stirred for 3 h, and the stirring speed was kept at 350 r.p.m during the whole magnetic stirring procedure. After the stirring, the mixture of NaCl powders, Al<sub>2</sub>O<sub>3</sub> fibers and Ti powders were poured into a vacuum filter, then washed using deionized water (DI water) to remove the NaCl powders. After washing several times, the remaining powder mixture was dried in an oven at 60 °C for 24 h. In addition, the NaCl solution after filtering was also dried at 60 °C in the oven for 3 days to recrystallize NaCl particles. The recycled NaCl particles were crushed in an agate mortal and sieved through 20 mesh for the next round of STS.

For comparison, 10 vol. %  $Al_2O_3$  fibers were dispersed directly in ethanol via ultrasound (VWR TM), followed by incorporation of Ti powders. And the speed of magnetic stirring was kept as 350 r.p.m. After 3 h, the mixture of  $Al_2O_3$  fibers and Ti powders were poured into vacuum filter directly. The remaining powder mixture was dried in an oven at 60 °C for 24 h. And Ti powder mixture containing 10 vol. %  $Al_2O_3$  fibers was obtained via NaCl STS. The optical photographs of the Ti powder mixture containing 10 vol. %  $Al_2O_3$  fibers via direct magnetic stirring and salt-templated strategy was compared (Fig. S1, supplementary materials).

### 2.2.2. Micro-material

SiC whiskers were also mixed with the Ti powder to confirm the feasibility of NaCl STS for the homogeneous mixing of Ti powders and micro-size fibers. The mixing procedure was the same as the procedures described above, afterwards, the Ti powder mixture containing 40 vol. % SiC whiskers was obtained after drying in the oven. Furthermore, the mixture of 20 vol. % Al<sub>2</sub>O<sub>3</sub> fiber on millimeter scale

and 20 vol. % SiC whiskers on micro-scale were also dispersed within Ti powders using the same NaCl STS procedure.

### 2.2.3. Nano-materials

In order to gain deeper insight on this approach to homogeneously distribute the mixtures with significantly different morphologies on nano-scale, graphene and  $SL-Ti_3C_2T_x$  powders were also distributed within Ti powders via NaCl STS. Here, considering the special morphologies of those nano-scale materials, the volume ratio of graphene and  $SL-Ti_3C_2T_x$  was selected as 10 vol. %, with the mixing procedure being the same as described above.

# 2.2.4. Sintering of bulk materials

Green compacts were prepared from the powder mixtures obtained via NaCl STS using a uniaxial hydraulic press under a pressure of 300 MPa for 5 min using a steel die with a diameter of 10 mm. The cold pressed compacts were then sintered via pressure less sintering at 1300 °C for 4 h in argon atmosphere with the heating/cooling rate of 5 K/min.

Before characterization, the surfaces of the as-sintered samples were ground with 400–4000-grid SiC sandpaper to remove the potential contaminated layers during the sintering. The samples were cut and embedded in water-free epoxy resin, then ground with SiC sandpaper and polished with 3  $\mu$ m, and subsequently 1  $\mu$ m diamond polishing compound (MetaDi, BUEHLER) with colloidal silica suspension (50 nm Alkaline, CLOEREN TECGNOLOGY GmbH).

# 2.2.5. NH<sub>4</sub>HCO<sub>3</sub> salt-templated strategy (STS)

 $40 \text{ vol.} \% \text{ Al}_2\text{O}_3$  fibers and Ti powders were mixed via the NH<sub>4</sub>HCO<sub>3</sub> STS. The volume of the NH<sub>4</sub>HCO<sub>3</sub> to Al<sub>2</sub>O<sub>3</sub> fibers was also selected to be 50:1. The Al<sub>2</sub>O<sub>3</sub> fibers were first dispersed in ethanol via ultrasound, then the NH<sub>4</sub>HCO<sub>3</sub> particles were added and the speed of the magnetic stirring was also kept at 350 r.p.m. Afterwards, Ti powders were introduced into the mixture of Al<sub>2</sub>O<sub>3</sub> fibers and NH<sub>4</sub>HCO<sub>3</sub> particles, then the powder mixture was moved to the filter paper for the vacuum filtering process, then calcined in an oven at  $60 \, ^{\circ}\text{C}$  for 3 days to evaporate the ethanol and decompose the NH<sub>4</sub>HCO<sub>3</sub> to remove the salt templates.

### 2.3. Characterization

The microstructures and phase distributions were characterized by field emission scanning electron microscopy (FE-SEM; Zeiss Merlin) for the powder mixture and polished surfaces of the as-sintered bulk materials. The remaining amount of NaCl particles of the powder mixture after washing and filtering using deionized water (DI water) was characterized via Inductively Coupled Plasma Optical Emission Spectrometry (ICP-OES, iCAP<sup>TM</sup> 7600 ICP-OES Analysator).

# 3. Results and discussion

Fig. 1a presents a schematic illustration of the NaCl salt-templated strategy (STS). Thereafter the Ti composites were obtained via cold pressing sintering (Fig. 1b). Obviously, the  $Al_2O_3$  fibers (Fig. 1c) have strong preference to agglomerate and entangle due to their large aspect ratio. Moreover, the angle of repose of NaCl particles (Fig. 1d) was determined to be  $40^{\circ}$ . The angle of repose is related to the free flowability properties of particulate materials in bulk forms [15]. Therefore, NaCl particles can act as templates with high free flowability. The remaining Ti powder mixture (Fig. 1e) is similar to a sponge structure owing to the interactions of 60 vol. %  $Al_2O_3$  fibers and the embedding of Ti powders, and no obvious agglomerates could be observed. Additionally, the microstructures of the as-obtained composite before and after sintering in Fig. 1f-g proof to be homogeneously distributed, demonstrating the feasibility of STS to mix short fibers on millimeter scale. To obtain a quantitative analysis on the distribution degree, Fig. 1g was divided into nine subsections. Here, the number of fibers was counted from the SEM image and the fiber within the subsection and those on the boundary line was counted as 1 and 0.5, respectively. And the distribution degree  $\alpha_f$  can be evaluated as follows [16]:

$$\alpha_{\rm f} = \exp\left[-\sqrt{\frac{\sum_{i=1}^{9} (X_i/X_{\rm average}-1)^2}{9}}\right] \tag{1}$$

where  $X_i$  is the number of Al<sub>2</sub>O<sub>3</sub> fibers positioned in the  $i_{th}$  area, and  $X_{average}$  is the average number of Al<sub>2</sub>O<sub>3</sub> fibers in the nine subsections.  $\alpha_f$  is the fiber distribution coefficient.  $\alpha_f = 1$  indicates that fibers are completely homogeneously distributed, and  $\alpha_f = 0$  indicates agglomeration of fibers. Here, the values of  $X_i$  and  $\alpha_f$  are summarized in Table 2. Considering the high distribution degree (0.894), the 60 vol. % Al<sub>2</sub>O<sub>3</sub> fibers were distributed rather homogeneously after the STS procedure.

An overview of the morphologies of the different materials confirms significant difference of morphologies between other components and Ti powder (Fig. 2 and Fig. 3a). Detailed information on the morphology of the components is summarized in Table 1, indicating the actual challenges to obtain homogeneous mixing of those components.

Clearly, after STS, the homogeneous distribution of the  $Al_2O_3$  fibers (40 vol. %) on millimeter scale within the powder mixture was confirmed (Fig. 3b). Additionally, the powder mixture obtained via NaCl STS (Fig. S1c-d) was more homogeneous than that via direct magnetic stirring (Fig. S1a-b). Moreover, 40 vol. % SiC whiskers were distributed homogeneously within the powder mixture (Fig. 3c), therefore, STS could be applied for the mixing of micro-materials. Furthermore, the uniform distribution of 20 vol. %  $Al_2O_3$  fibers and 20 vol. % SiC whiskers within Ti powder mixture can also be observed (Fig. 3d), demonstrating the wide feasibility of STS in the mixing of components on millimeter and/or micro-scale.

As known, when the particle size reaches nano-scale, the agglomeration effect increases strongly, and the mutual attraction of the particles in the agglomerate increases significantly [17], hence, more difficulties in dispersion occur, leading to a strong agglomeration effect during the applications. Graphene and MXene nano-sheets with large aspect ratio are easily entangled and bonded together to form larger agglomerates (Fig. 2e-h). Here, 10 vol. % graphene nano-sheets were characterized to be dark phases and homogeneously distributed within Ti powder mixture (Fig. 3e), and no obvious agglomerates were observed comparing with the agglomerates of graphene powder (Fig. 2e-f).

Moreover, as shown in Fig. 3f, 10 vol. % graphene-like  $SL-Ti_3C_2T_x$  sheets distributed well within Ti powders after STS comparing to the serious agglomeration of  $SL-Ti_3C_2T_x$  powders (approx. 100-200  $\mu$ m, Fig. 2g-h). Note that, the parameters of NaCl STS, such as the selection of salts, particle size of salts, the ratio of the salts to the components, stirring speed etc, should be optimized in future works, especially for the nano-components (graphene,  $SL-Ti_3C_2T_x$  etc.) Even though, STS is still applicable for the homogeneous mixing of the components with morphologies ranging from millimeter to nano-scale.

To illustrate the mixing mechanism, Ti powder mixture containing 40 vol. % Al<sub>2</sub>O<sub>3</sub> fibers was repeated, but NaCl particles remained. As shown in Fig. 4a-b, NaCl particles distributed well between Ti powders and Al<sub>2</sub>O<sub>3</sub> fibers, and retained the distance/space between Al<sub>2</sub>O<sub>3</sub> fibers and Ti powders. As a result, the Al<sub>2</sub>O<sub>3</sub> fibers were separated to prevent the agglomeration and dispersed well. In addition, the NaCl particle could act as the milling agents during the magnetic stirring considering its excellent free flowability, which will also accelerate the mixing process. As illustrated in Fig. 4c, the components were first dispersed homogeneously using ultrasonic, NaCl particles were introduced to retain the distance/space of the dispersed components to avoid the re-agglomeration after the initial ultrasonic and the following magnetic stirring procedure. Furthermore, with respect to the micromechanics between the NaCl particles and the components, as shown in the enlarged zone, with the rotation of the magnetic stirrer, the NaCl particles in different positions will move in some slightly different directions, thus acting as 'micro-ball milling agents' to separate the components.

Additionally, regarding the Ti powder mixture containing 40 vol. %  $Al_2O_3$  fibers, after washing and drying, the remaining  $Na^+$  has been determined to be  $0.0056 \pm 0.0007$  wt. % via ICP-OES. Therefore, the NaCl templates have been almost completely removed by water washing, thus no influence of the salt is expected for further applications. The recycled NaCl crystals were collected to be 50.438 g, which is 99.3 wt. % of the initially introduced NaCl salts (50.779 g), and the loss of the NaCl salt can be almost ignored, illustrating the low cost of the NaCl STS.

Fig. 5 presents the microstructure of polished surfaces of the as-sintered Ti composites. The monolithic Ti material was obtained with high density although some tiny pores existed after sintering (Fig. 5a). Additionally, as shown in Fig. 5b-d, 40 vol. % short Al<sub>2</sub>O<sub>3</sub> fibers and 40 vol. % SiC whiskers as well as 20 vol. % Al<sub>2</sub>O<sub>3</sub> fibers and 20 vol. % SiC whiskers were still distributed homogeneously within the Ti composites although the reactions between Ti and the fibers/whiskers occurred during the sintering. Moreover, regarding the composites containing 10 vol. % graphene (Fig. 5e), obviously, the determined dark gray graphene sheets were distributed relatively homogeneously although slight agglomerates were observed because of the high amount of the graphene. Furthermore, 10 vol. % SL-Ti<sub>3</sub>C<sub>2</sub>T<sub>x</sub> within Ti composite was observed as dark gray phases, and remained separated and distributed homogeneously (Fig. 5f). Based on all above, the microstructure of powder mixture obtained via STS remained homogeneous after the sintering, demonstrating the stability of the homogeneity of the powder mixture obtained via STS.

Moreover, STS can be further developed to various approaches using different salts, here, as an example, NH<sub>4</sub>HCO<sub>3</sub> STS also worked well with the homogeneous mixing of 40 vol. % Al<sub>2</sub>O<sub>3</sub> fibers and Ti powders (Fig. S2), and avoided the washing procedure using DI water, therefore, STS can be presented in various forms to solve different challenges existing in various areas.

### 4. Conclusion

In summary, for the first time, titanium composites containing homogeneously distributed multi components (Al<sub>2</sub>O<sub>3</sub> fiber, SiC whisker, graphene and MXene) with morphologies ranging from millimeter to nano- scale, were achieved by a simple and environmentally friendly salt-templated strategy (STS) combined with a vacuum filtering process to remove and recycle the salt templates. And this approach is by virtue of the retained space/distance between different components and the 'ball milling agents' effects via salt templates. The homogeneity of as-obtained composites was characterized and confirmed. Furthermore, the STS can be scaled up to industrial scale by simply increasing the batch size or making the process continuous considering the easy operation, low cost of STS. More importantly, the versatility of STS can be universally applied on various scientific or industrial fields without the consideration of various factors, such as the functional groups on the graphene, SL-Ti<sub>3</sub>C<sub>2</sub>T<sub>x</sub>. Therefore, this strategy offers the possibility for not just some specified materials but the application for various kinds of materials in different fields.

# Acknowledgements

This work was supported by the China Scholarship Council of China [grant numbers: 201808440373]. The authors would like to thank Dr. E. Wessel, Dr. D. Grüner for the microstructural investigations via SEM. Supports from Prof. R. Schwaiger and Dr. M. Müller are highly acknowledged.

# References

- [1] T.K. Das, P. Ghosh, N.C. Das, Preparation, development, outcomes, and application versatility of carbon fiber-based polymer composites: a review, Adv. Compos. Hybrid. Mater. 2 (2019) 214-233.
- [2] A. Dash, J. Malzbender, K. Dash, M. Rasinski, R. Vaßen, O. Guillon, J. Gonzalez-Julin, Compressive creep of SiC whisker/Ti<sub>3</sub>SiC<sub>2</sub> composites at high temperature in air, J. Am. Ceram. Soc. 103 (2020) 5952-5965.
- [3] Q. Zhang, J. Gu, S. Wei, M. Qi, Differences in Dry Sliding Wear Behavior between Al–12Si–CuNiMg Alloy and Its Composite Reinforced with Al<sub>2</sub>O<sub>3</sub> Fibers, Materials 12 (2019) 1749.
- [4] D.G. Papageorgiou, Z.L. Li, M.F. Liu, I.A. Kinloch, R.J. Young, Mechanisms of mechanical reinforcement by graphene and carbon nanotubes in polymer nanocomposites, Nanoscale 12 (2020) 2228-2267
- [5] J. Banerjee, A.S. Panwar, K. Mukhopadhyay, A.K. Saxena, A.R. Bhattacharyya, Deagglomeration of multi-walled carbon nanotubes via an organic modifier: structure and mechanism, Phys. Chem. Chem. Phys. 17 (2015) 25365-25378

- [6] O.T. Picot, V.G. Rocha, C. Ferraro, N. Ni, E, D'Elia, S. Meille, J. Chevalier, T. Saunders, T. Peijs, M.J. Reece, E. Sai, Using graphene networks to build bioinspired self-monitoring ceramics, Nat. Commun. 8 (2017) 14425.
- [7] K.S. Munir, Y.C. Li, D. Liang, M. Qian, W. Xu. C. Wen, Effect of dispersion method on the deterioration, interfacial interactions and re-agglomeration of carbon nanotubes in titanium metal matrix composites, Mater. Des. 88 (2015) 138-148.
- [8] T.L. Han, J.J. Li, N.Q. Zhao, C.N. He, Microstructure and properties of copper coated graphene nanoplates reinforced Al matrix composites developed by low temperature ball milling, Carbon 159 (2020) 311-323.
- [9] S.J. Yoo, S.H. Han, W.J. Kim, Strength and strain hardening of aluminum matrix composites with randomly dispersed nanometer-length fragmented carbon nanotubes, Scr. Mater. 68 (2013) 711-714.
- [10] B.Y. Conde, J.F. Despois, R. Goodall, A. Marmottant, L. Salvo, C.S. Marchi, A. Mortensen, Replication Processing of Highly Porous Materials, Adv. Eng. Mater. 8 (2006) 795-803.
- [11] G. Wang, S.K. Kim, M.C. Wang, T.S. Zhai, S. Munukutla, G.S. Girolami, P.J. Sempsrott, S.W. Nam, P.V. Braun, J.W. Lyding, Enhanced Electrical and Mechanical Properties of Chemically Cross-Linked Carbon-Nanotube-Based Fibers and Their Application in High-Performance Supercapacitors, ACS Nano 14 (2019) 632-639.
- [12] J.H. Kim, J.Y. Hwang, H.R. Hwang, H.S. Kim, J.H. Lee, J.W. Seo, U.S. Shin, S.H. Lee, Simple and cost-effective method of highly conductive and elastic carbon nanotube/polydimethylsiloxane composite for wearable electronics, Sci. Rep. 8 (2018) 1375.
- [13] X.J. Cui, W. Li, P. Ryabchuk, K. Junge, M. Beller, Bridging homogeneous and heterogeneous catalysis by heterogeneous single-metal-site catalysts, Nat. Catal. 1 (2018) 385-397.
- [14] N. Kleger, M. Cihova, K. Masania, A.R. Studart, J.F. Löffler, 3D Printing of Salt as a Template for Magnesium with Structured Porosity, Adv. Mater. 31 (2019) e1903783.
- [15] T.F. Teferra, Handbook of Farm, Dairy and Food Machinery Engineering, 2019, pp. 45-89.
- [16] G.X. Ji, G.Q. Xiong, X.Q. Peng, S.P. Wang, C. Wang, K.K. Sun, L. Zeng, Quantitative Evaluation of Carbon Fiber Dispersion in Amorphous Calcium Silicate Hydrate-Based Contact-Hardening Composites, Molecules 26 (2021) 726.
- [17] E.T. Thostenson, Z. Ren, T.W. Chou, Advances in the science and technology of carbon nanotubes and their composites: a review, Compos. Sci. Technol. 61 (2001) 1899-1912.

# **a** Salt-templated strategy

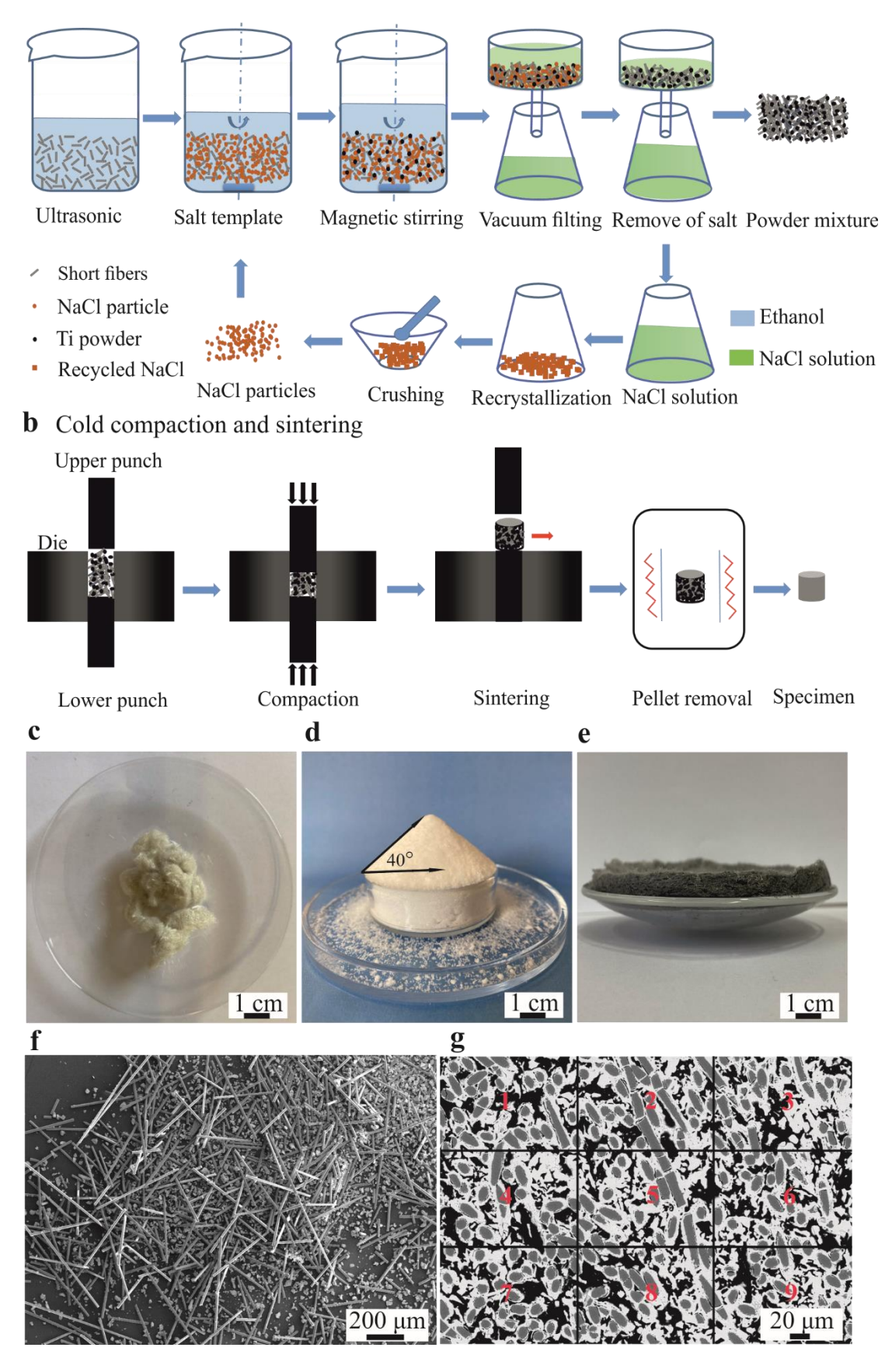


Fig. 1. The salt-templated strategy process and the as-obtained composites. a) The schematic illustration of the NaCl salt-templated strategy. b) Cold compaction and sintering of the composites. The optical

photographs of c) de-sized  $Al_2O_3$  fibers, d) commercial NaCl particles, e) Ti powder mixture containing 60 vol. %  $Al_2O_3$  fibers, and corresponding SEM image of f) powder mixture and g) bulk material after sintering. The number of  $Al_2O_3$  fibers positioned in the  $i_{th}$  area was counted. Here, the number of fibers was counted from the SEM image and the fiber within the subsection and those on the boundary line was counted as 1 and 0.5, respectively.

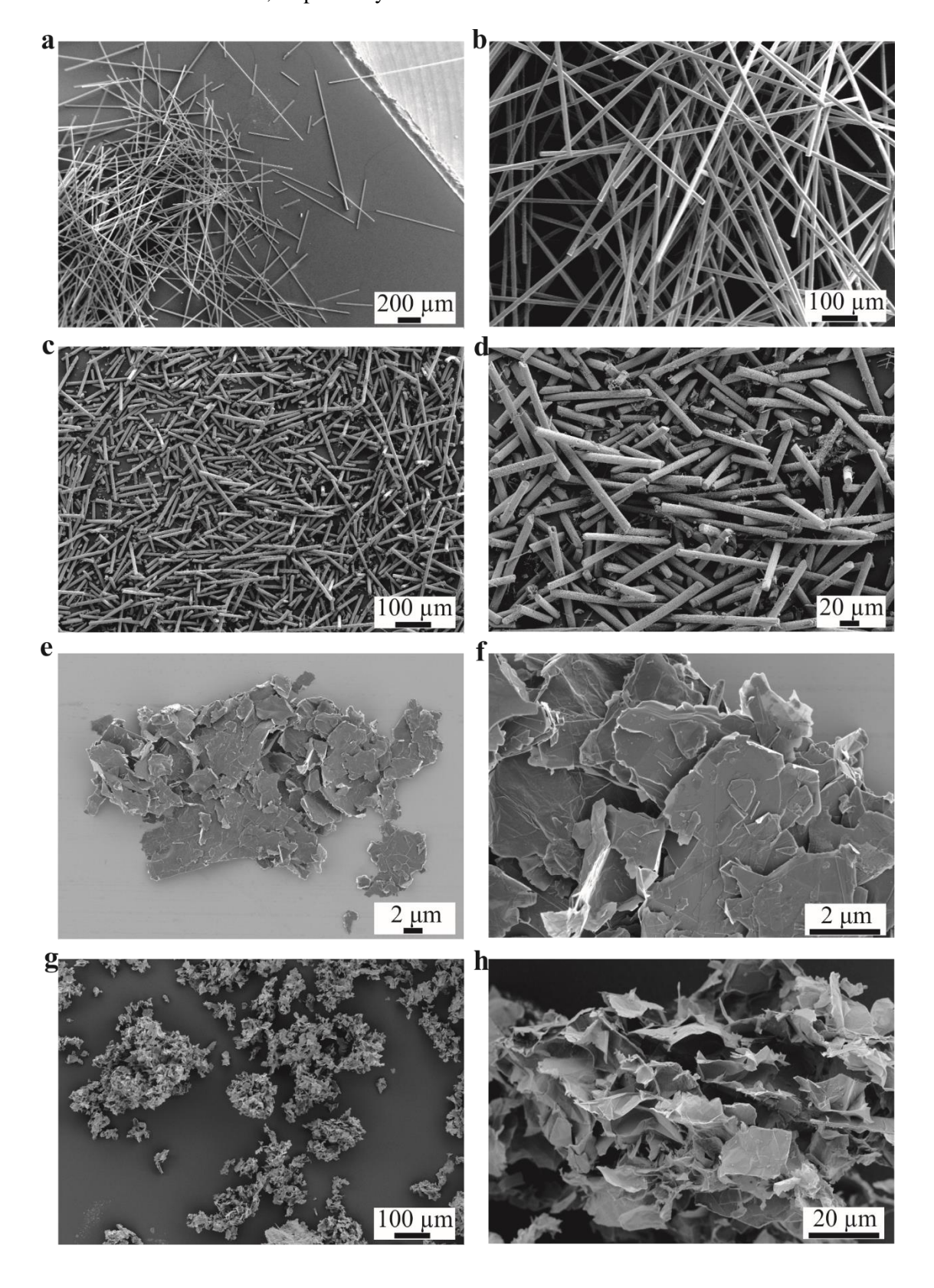


Fig. 2. The raw materials. The SEM images of a-b) de-sized short  $Al_2O_3$  fibers, c-d) commercial SiC whiskers, e-f) commercial graphene, g-h) as-synthesized  $SL-Ti_3C_2T_x$ .

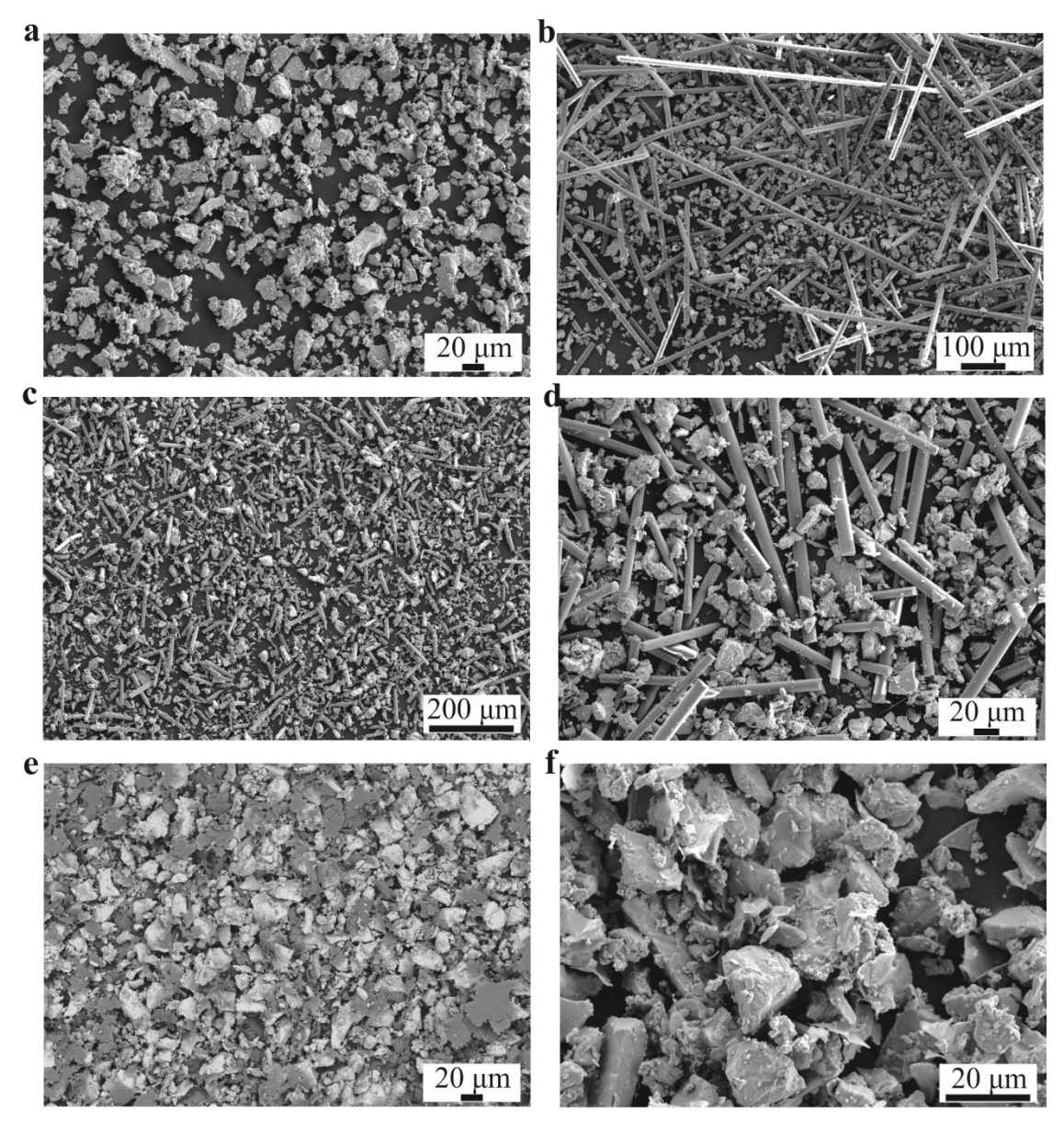


Fig. 3. The Ti powder mixtures obtained via NaCl STS. The SEM images of (a) Ti powder and Ti powder mixtures containing b) 40 vol. % short  $Al_2O_3$  fibers, c) 40 vol. % SiC whiskers, d) 20 vol. % short  $Al_2O_3$  fibers and 20 vol. % SiC whiskers, e) 10 vol. % graphene, and f) 10 vol. % SL-Ti<sub>3</sub>C<sub>2</sub>T<sub>x</sub>.

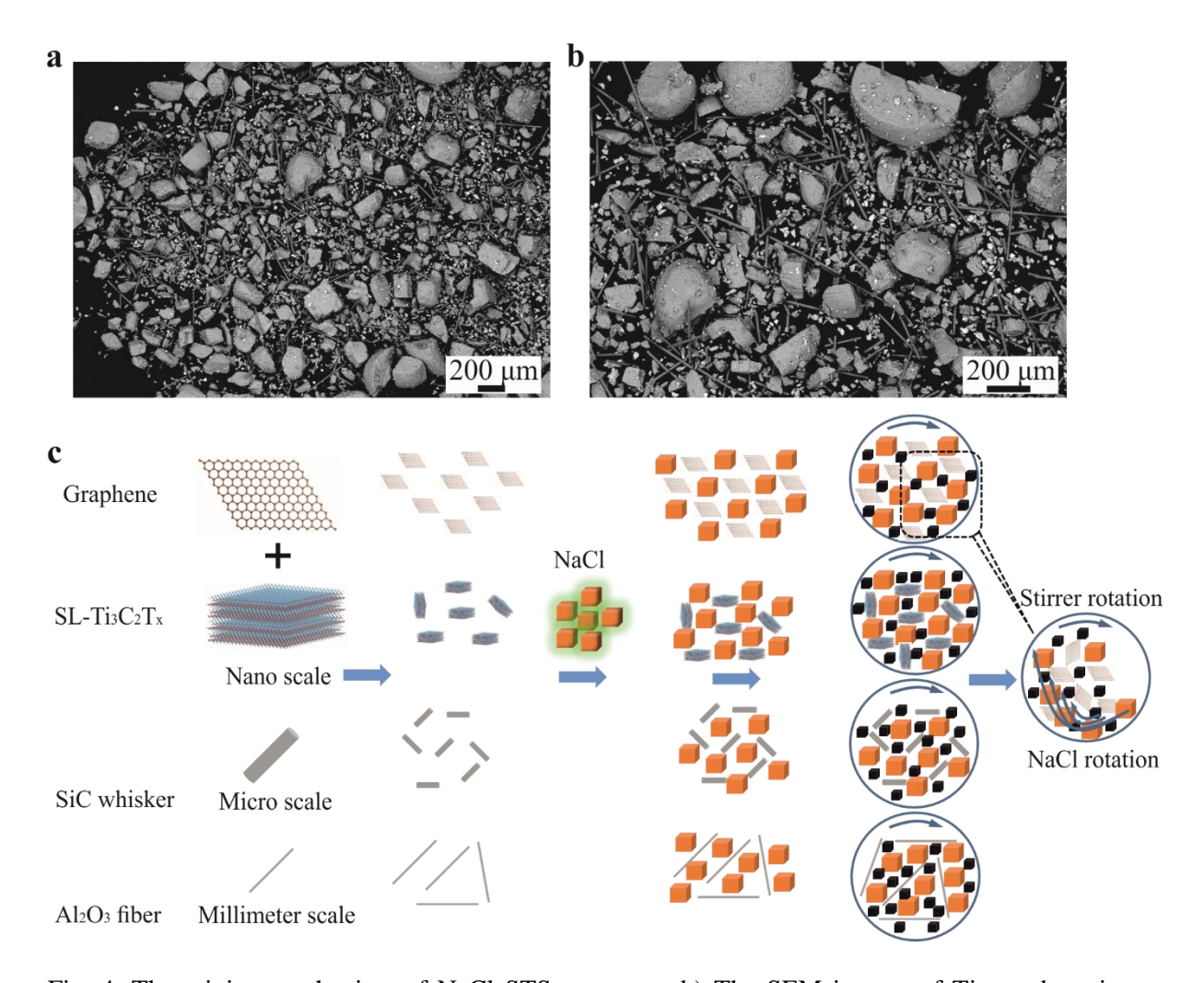


Fig. 4. The mixing mechanism of NaCl STS process. a-b) The SEM images of Ti powder mixture containing 40 vol. % short  $Al_2O_3$  fibers and NaCl salt templates and c) The schematic illustration of the mixing mechanism for NaCl salt-templated strategy. The 'ball milling agents' effects due to the micromechanics from NaCl templates were shown in the enlarged zone of Fig. 4c.

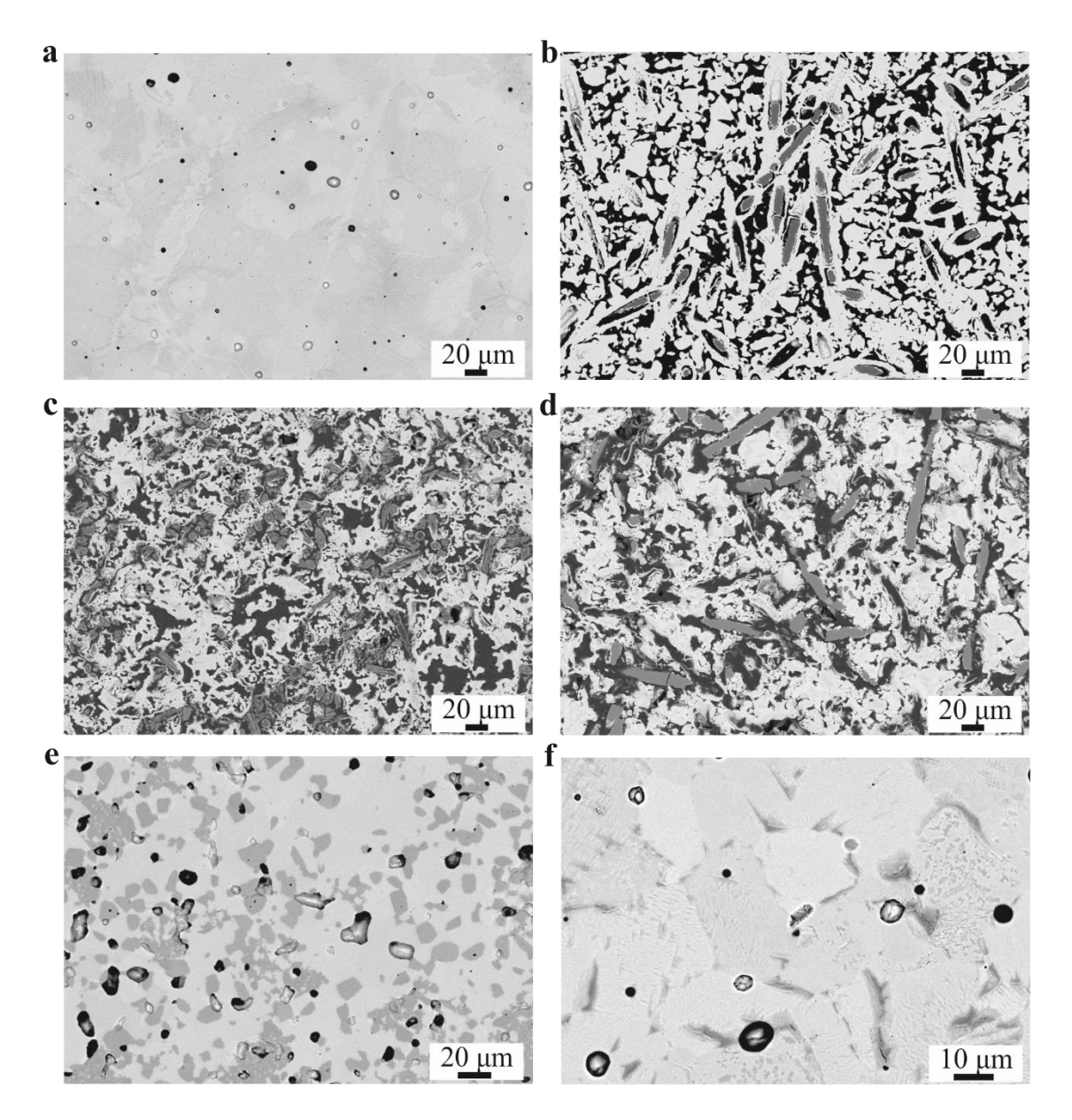


Fig. 5. The as-sintered Ti composites from the powder mixtures obtained via NaCl STS process. The SEM images of the polished surfaces of a) bulk Ti composite, Ti composites containing b) 40 vol. %  $Al_2O_3$  short fibers, c) 40 vol. % SiC whiskers, d) 20 vol. %  $Al_2O_3$  short fibers and 20 vol. % SiC whiskers, e) 10 vol. % graphene, and f) 10 vol. % SL-Ti<sub>3</sub>C<sub>2</sub>T<sub>x</sub> after pressure less sintering at 1300 °C for 4 h.

Table 1 Summary of the morphology of the components and experimental parameters for NaCl salt-templated strategy.

Components		Length (μm)	Diameter/thickness (μm)	Aspect/surface ratio	Volume ratio (%)
Millimeter scale	Al <sub>2</sub> O <sub>3</sub> fiber	~1000	~10	~100	40, 60
Micro scale	SiC whisker	~100	~10	~10	40
Nano scale	Graphene	~5	~0.006	~833	10
	MXene	~10	~0.008	~1250	10

Table 2 Summary of the number of  $Al_2O_3$  fibers positioned in the  $i_{th}$  area and distribution degree of Ti composites containing 60 vol. %  $Al_2O_3$  fibers.

$X_{\rm i}$	1	2	3	4	5	6	7	8	9
	24.5	24.5	22	21		23	25	24.5	23
$lpha_{ m f}$					0.894				